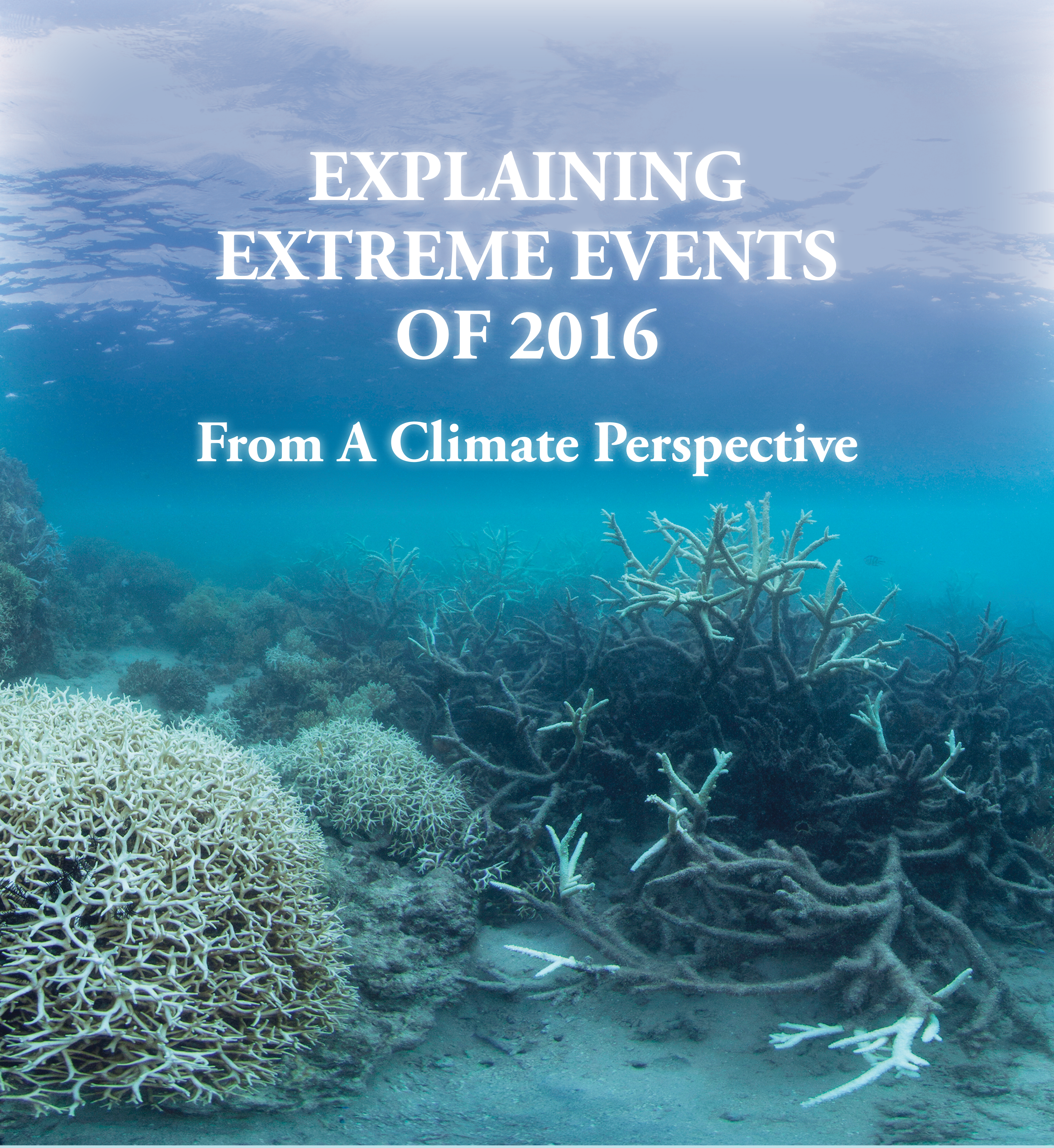

EXPLAINING EXTREME EVENTS OF 2016

From A Climate Perspective

Special Supplement to the
Bulletin of the American Meteorological Society
Vol. 99, No. 1, January 2018

EXPLAINING EXTREME EVENTS OF 2016 FROM A CLIMATE PERSPECTIVE

Editors

Stephanie C. Herring, Nikolaos Christidis, Andrew Hoell, James P. Kossin, Carl J. Schreck III, and Peter A. Stott

Special Supplement to the

Bulletin of the American Meteorological Society

Vol. 99, No. 1, January 2018

American Meteorological Society

CORRESPONDING EDITOR:

Stephanie C. Herring, PhD
NOAA National Centers for Environmental Information
325 Broadway, E/CC23, Rm 1B-131
Boulder, CO 80305-3328
E-mail: stephanie.herring@noaa.gov

COVER CREDIT:

©The Ocean Agency / XL Catlin Seaview Survey / Chrisophe Bailhache—A panoramic image of coral bleaching at Lizard Island on the Great Barrier Reef, captured by The Ocean Agency / XL Catlin Seaview Survey / Christophe Bailhache in March 2016.

HOW TO CITE THIS DOCUMENT

Citing the complete report:

Herring, S. C., N. Christidis, A. Hoell, J. P. Kossin, C. J. Schreck III, and P. A. Stott, Eds., 2018: Explaining Extreme Events of 2016 from a Climate Perspective. *Bull. Amer. Meteor. Soc.*, **99** (1), S1–S157.

Citing a section (example):

Quan, X.W., M. Hoerling, L. Smith, J. Perlwitz, T. Zhang, A. Hoell, K. Wolter, and J. Eischeid, 2018: Extreme California Rains During Winter 2015/16: A Change in El Niño Teleconnection? [in "Explaining Extreme Events of 2016 from a Climate Perspective"]. *Bull. Amer. Meteor. Soc.*, **99** (1), S54–S59, doi:10.1175/BAMS-D-17-0118.1.

EDITORIAL AND PRODUCTION TEAM

Riddle, Deborah B., Lead Graphics Production, NOAA/NESDIS National Centers for Environmental Information, Asheville, NC

Love-Brotak, S. Elizabeth, Graphics Support, NOAA/NESDIS National Centers for Environmental Information, Asheville, NC

Veasey, Sara W., Visual Communications Team Lead, NOAA/NESDIS National Centers for Environmental Information, Asheville, NC

Fulford, Jennifer, Editorial Support, Telesolv Consulting LLC, NOAA/NESDIS National Centers for Environmental Information, Asheville, NC

Griffin, Jessicca, Graphics Support, Cooperative Institute for Climate and Satellites-NC, North Carolina State University, Asheville, NC

Misch, Deborah J., Graphics Support, Telesolv Consulting LLC, NOAA/NESDIS National Centers for Environmental Information, Asheville, NC

Osborne, Susan, Editorial Support, Telesolv Consulting LLC, NOAA/NESDIS National Centers for Environmental Information, Asheville, NC

Sprain, Mara, Editorial Support, LAC Group, NOAA/NESDIS National Centers for Environmental Information, Asheville, NC

Young, Teresa, Graphics Support, Telesolv Consulting LLC, NOAA/NESDIS National Centers for Environmental Information, Asheville, NC

TABLE OF CONTENTS

ABSTRACT—Stephanie C. Herring, Nikolaos Christidi, Andrew Hoell, James P. Kossin, Carl J. Schreck III, and Peter A. Stott

This sixth edition of explaining extreme events of the previous year (2016) from a climate perspective is the first of these reports to find that some extreme events were not possible in a preindustrial climate. The events were the 2016 record global heat, the heat across Asia, as well as a marine heat wave off the coast of Alaska. While these results are novel, they were not unexpected. Climate attribution scientists have been predicting that eventually the influence of human-caused climate change would become sufficiently strong as to push events beyond the bounds of natural variability alone. It was also predicted that we would first observe this phenomenon for heat events where the climate change influence is most pronounced. Additional retrospective analysis will reveal if, in fact, these are the first events of their kind or were simply some of the first to be discovered.

Last year, the editors emphasized the need for additional papers in the area of "impacts attribution" that investigate whether climate change's influence on the extreme event can subsequently be directly tied to a change in risk of the socio-economic or environmental impacts. Several papers in this year's report address this challenge, including Great Barrier Reef bleaching, living marine resources in the Pacific, and ecosystem productivity on the Iberian Peninsula. This is an increase over the number of impact attribution papers than in the past, and are hopefully a sign that research in this area will continue to expand in the future.

Other extreme weather event types in this year's edition include ocean heat waves, forest fires, snow storms, and frost, as well as heavy precipitation, drought, and extreme heat and cold events over land. There were a number of marine heat waves examined in this year's report, and all but one found a role for climate change in increasing the severity of the events. While human-caused climate change caused China's cold winter to be less likely, it did not influence U.S. storm Jonas which hit the mid-Atlantic in winter 2016.

As in past years, the papers submitted to this report are selected prior to knowing the final results of whether human-caused climate change influenced the event. The editors have and will continue to support the publication of papers that find no role for human-caused climate change because of their scientific value in both assessing attribution methodologies and in enhancing our understanding of how climate change is, and is not, impacting extremes. In this report, twenty-one of the twenty-seven papers in this edition identified climate change as a significant driver of an event, while six did not. Of the 131 papers now examined in this report over the last six years, approximately 65% have identified a role for climate change, while about 35% have not found an appreciable effect.

Looking ahead, we hope to continue to see improvements in how we assess the influence of human-induced climate change on extremes and the continued inclusion of stakeholder needs to inform the growth of the field and how the results can be applied in decision making. While it represents a considerable challenge to provide robust results that are clearly communicated for stakeholders to use as part of their decision-making processes, these annual reports are increasingly showing their potential to help meet such growing needs.

8. THE HIGH LATITUDE MARINE HEAT WAVE OF 2016 AND ITS IMPACTS ON ALASKA

John E. Walsh, Richard L. Thoman, Uma S. Bhatt, Peter A. Bieniek, Brian Brettschneider, Michael Brubaker, Seth Danielson, Rick Lader, Florence Fetterer, Kris Holderied, Katrin Iken, Andy Mahoney, Molly McCammon, and James Partain

The 2016 Alaska marine heat wave was unprecedented in terms of sea surface temperatures and ocean heat content, and CMIP5 data suggest human-induced climate change has greatly increased the risk of such anomalies.

Earth System Observations. The Gulf of Alaska (GOA) and Bering Sea have been anomalously warm for several years with the warmth peaking in 2016. As a consequence of the high marine heat content (HC) and SSTs, coastal areas of Alaska had their warmest winter–spring of record in 2016 (Walsh et al. 2017) and earliest river ice breakup for multiple Alaska rivers (www.weather.gov/aprfc/breakupDB). Observed marine warmth, impacts on the marine ecosystem, and an attribution analysis using CMIP5 models are presented here.

The marine heat wave was first noted over deep waters of the northeastern Pacific Ocean in January 2014 (Freeland 2014; Bond et al. 2015); anomalous temperatures at coastal GOA stations arrived variously between January and June. Warm temperature anomalies were confined to the top 100 meters until late 2014, after which they penetrated to depths of 300 meters and reached strengths greater than 2 standard deviations (Roemmich and Gilson 2009).

AFFILIATIONS: Walsh and Brettschneider—Alaska Center for Climate Assessment and Policy, University of Alaska, Fairbanks, Alaska; Thoman—NOAA/National Weather Service Alaska, Fairbanks, Alaska; Bhatt—Geophysical Institute, and Department of Atmospheric Sciences, University of Alaska, Fairbanks, Alaska; Mahoney—Geophysical Institute, University of Alaska, Fairbanks, Alaska; Lader—International Arctic Research Center, University of Alaska, Fairbanks, Alaska; Bieniek—Alaska Climate Science Center, University of Alaska, Fairbanks, Alaska; Brubaker—Alaska Native Tribal Health Consortium, Anchorage, Alaska; Danielson and Iken —College of Fisheries and Ocean Sciences, University of Alaska, Fairbanks, Alaska; Fetterer—NSIDC and NOAA/NESDIS National Centers for Environmental Information, Boulder, Colorado; Holderied—NOAA/National Ocean Service, National Centers for Coastal Ocean Science, Seldovia, Alaska; McCammon—Alaska Ocean Observing System, Anchorage, Alaska; Partain—NOAA/NESDIS National Centers for Environmental Information, Anchorage, Alaska

DOI:10.1175/BAMS-D-17-0105.1

A supplement to this article is available online (10.1175/BAMS-D-17-0105.2)

The consensus of previous studies is that atmospheric circulation anomalies played a key role in initiating and maintaining the North Pacific "blob" of warm water (Bond et al. 2015). Unusually high pressure south of the Gulf of Alaska reduced heat loss to the atmosphere and also reduced cold advection over the region. Forcing of the atmospheric anomalies has been linked to SST anomalies in the western tropical Pacific Ocean (Seager et al. 2015) and to decadal-scale modes of North Pacific Ocean variability (Di Lorenzo and Mantua 2016). Lee et al. (2015) have argued that sea ice anomalies also contributed to the atmospheric circulation anomalies in 2013/14. By contrast, the winter of 2015/16 was characterized by negative sea level pressure anomalies of more than 12 hPa centered in the eastern Bering Sea (Fig. ES8.1d). The associated northward airflow evident throughout the depth of the atmosphere (Fig. ES8.1b) likely drove lingering heat from the blob into the GOA and Bering Sea regions. An unusually deep Aleutian low is a typical feature of the El Niño conditions that characterized early 2016 (Walsh et al. 2017).

The positive HC anomalies (Fig. 8.1a) reached an extreme in 2016 for the GOA and Bering Sea (Figs. 8.1d,e), with most of the region ranking in the top five warmest HCs of record (Fig. ES8.2a). Oceanic temperatures are from GODAS (Saha et al. 2006), NCEP's high-resolution ocean analysis. HC was calculated by integrating ocean temperature (°C) from the surface to 300 meters or the bottom of each model water column. This value was then divided by the depth of its respective water column, the 1981–2010 mean was removed, and the quantity was normalized to allow comparison between the Bering Sea (51°–64.5°N, 180°–160°W) and GOA (50°–60°N, 150°–130°W) regions (Figs. 8.1d,e).

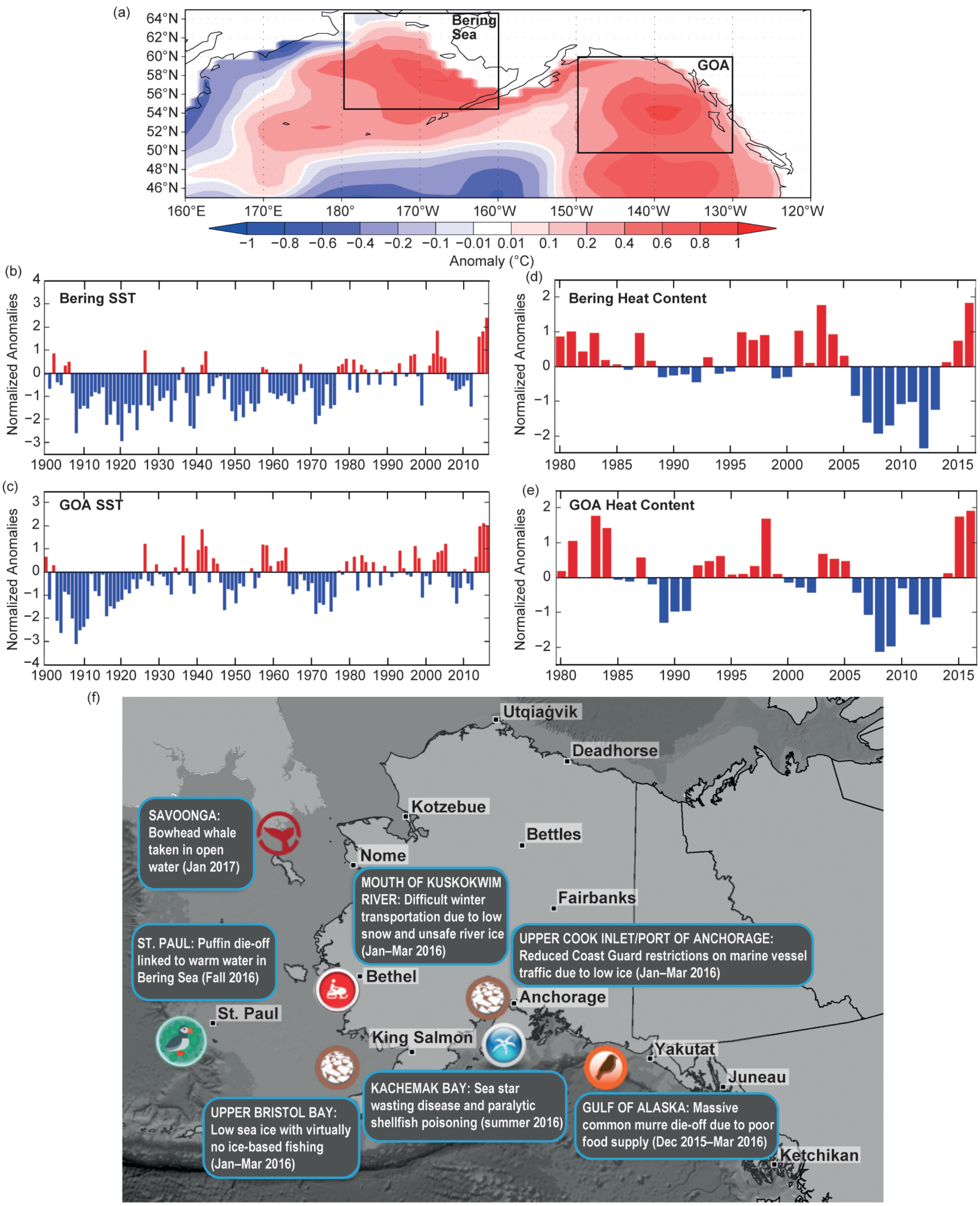

Fig. 8.1. (a) Jan–Dec 2016 ocean heat content anomaly (°C) from the surface to 300 m or bottom of ocean column. Boxes outline GOA and Bering Sea regions. Normalized area-weighted SST anomalies for (b) Bering Sea and (c) GOA. Normalized area-weighted heat content anomalies for (d) Bering Sea and (e) GOA. (f) Select impacts of 2016 marine heat in Alaska waters.

Normalized SST anomalies from 1900 provide context for the anomalies. The 2016 SSTs were the warmest on record for the Bering Sea and the second warmest in the GOA (Figs. 8.1b,c) where 2015 was warmest. SSTs were anomalously warm starting in 2012 (Weller et al. 2015), and most of the GOA and

Bering Sea ranked in the top five SSTs of record (Fig. ES8.2b). SST data are from NOAA's Extended Reconstructed Sea Surface Temperature dataset, version 4 (Huang et al. 2014), and anomalies use the 1981–2010 mean. Negative anomalies greater than 2 sigma are evident in both regions from 2006–13.

The warming was primarily confined to the inner GOA shelf in September 2014, suggesting that heat was advected along-shore within the Alaska Coastal Current. By spring 2015 the shelf was uniformly warm and water remained 1°–2°C warmer than normal through September 2016. This heat was accompanied by surface mixed layer shoaling and a strengthening of the near-surface stratification, impacting nutrient availability and the ecosystem.

Impacts. Ecological and societal impacts of the 2016 marine heat wave are complex but unequivocal. Some marine ecological impacts resulted from the multiyear nature of the marine heat wave, so cannot be attributed solely to the 2016 event.

The consequences of this persistent warming were felt through the entire marine food web. The warm conditions favored some phytoplankton species, and one of the largest harmful algal blooms on record reached the Alaska coast in 2015 (Peterson et al. 2016a). Kachemak Bay had uncommon paralytic shellfish poisoning events and oyster farm closures in 2015 and 2016. Copepods, the crustaceans that form the cornerstone of the open ocean food web, had a higher abundance of smaller species, which provide less nutritious food source to higher trophic levels, including forage fish. The occurrence of more southern copepod species in the GOA likely resulted from the anomalous warmth (Kintisch 2015; Peterson et al. 2016b).

The dramatic mortality events in seabird species such as common murres (*Uria aalge*) in 2015/16 (tens of thousands of dead birds counted) were attributed to starvation and presumed to be a result of warming-induced effects on food supply (H. Renner 2017, U.S. Fish and Wildlife Service, personal communication). Increased occurrences of diseases were also observed, including sea star wasting disease, first recognized in Kachemak Bay in 2015. (K. Iken 2017, personal observations; Fig. 8.1f).

Over 100 observations of impacts on communities across Alaska were posted to the Local Environmental Observer (LEO) network (http://leonetwork.org) between October 2013 and December 2016. These impacts relate to changes in the acquisition, preservation, quality, and quantity of wild foods. Local observers noted changes in seasonality, weather, ocean conditions, plants, and wildlife, which challenge people engaged in subsistence and commercial activities with increased variability and uncertainty. The lack of winter sea ice in western Alaska delayed or prevented ice-based harvesting of fish, crab, seal, and whale. For shellfish harvests, the warm waters translated into persistent high levels of harmful algae across the GOA and North Pacific as far west as the Aleutian Islands, with concerns about food safety extending to the Bering Strait.

Attribution. The role of anthropogenic climate change in the marine heat wave of 2016 was assessed through an evaluation of CMIP5 model output. Attribution was estimated by comparing SSTs and HC in 60-year segments (to resolve relevant decadal variability such as the Pacific decadal oscillation; PDO) from present and preindustrial climate simulations. Five CMIP5 models were selected (see online supplement material; Walsh et al. 2017b, manuscript submitted to *Environ. Modell. Software*): CCSM4, GFDL-CM3, GISS-E2-R, IPSL-CM5A-LR, and MRI-CGCM3. The models' trends of SST over the 1900–2005 historical simulations ranged from 0.27° to 0.52°C century^{-1} (mean = 0.41°C) for the Bering Sea and 0.22° to 0.90°C century^{-1} (mean = 0.46°C) for the GOA. The corresponding observational values from Figs. 8.1b,c are 0.70° and 0.84°C century^{-1} for the Bering Sea and GOA. If the models' century-scale trends represent the anthropogenic forcing signal, then one may argue that the larger values of the observed trends are partially attributable to internal variability.

For the attribution analysis, the present climate period is centered on 2016 and incorporates the historical simulation (1987–2005) and RCP8.5 (2006–46), which is the current trajectory of climate forcing, while the preindustrial climate incorporates a random 60-year period from each model. Monthly HC was calculated using ocean potential temperatures with a procedure similar to that used for GODAS. The SSTs and HCs were then interpolated to the GODAS grid, annual averages were computed, and area-weighted averages were extracted over the Bering Sea and GOA. This yielded 60-year time series for each region, model, and variable (present and preindustrial).

Annual values of SST and HC are warmer in GOA than the Bering Sea. Normalized anomalies using a 1987–2016 base period were used to account for differences in means. For SST and HC the present climate has increasing trends while the preindustrial does not (Figs. 8.2a,b). In all cases the preindustrial climate is

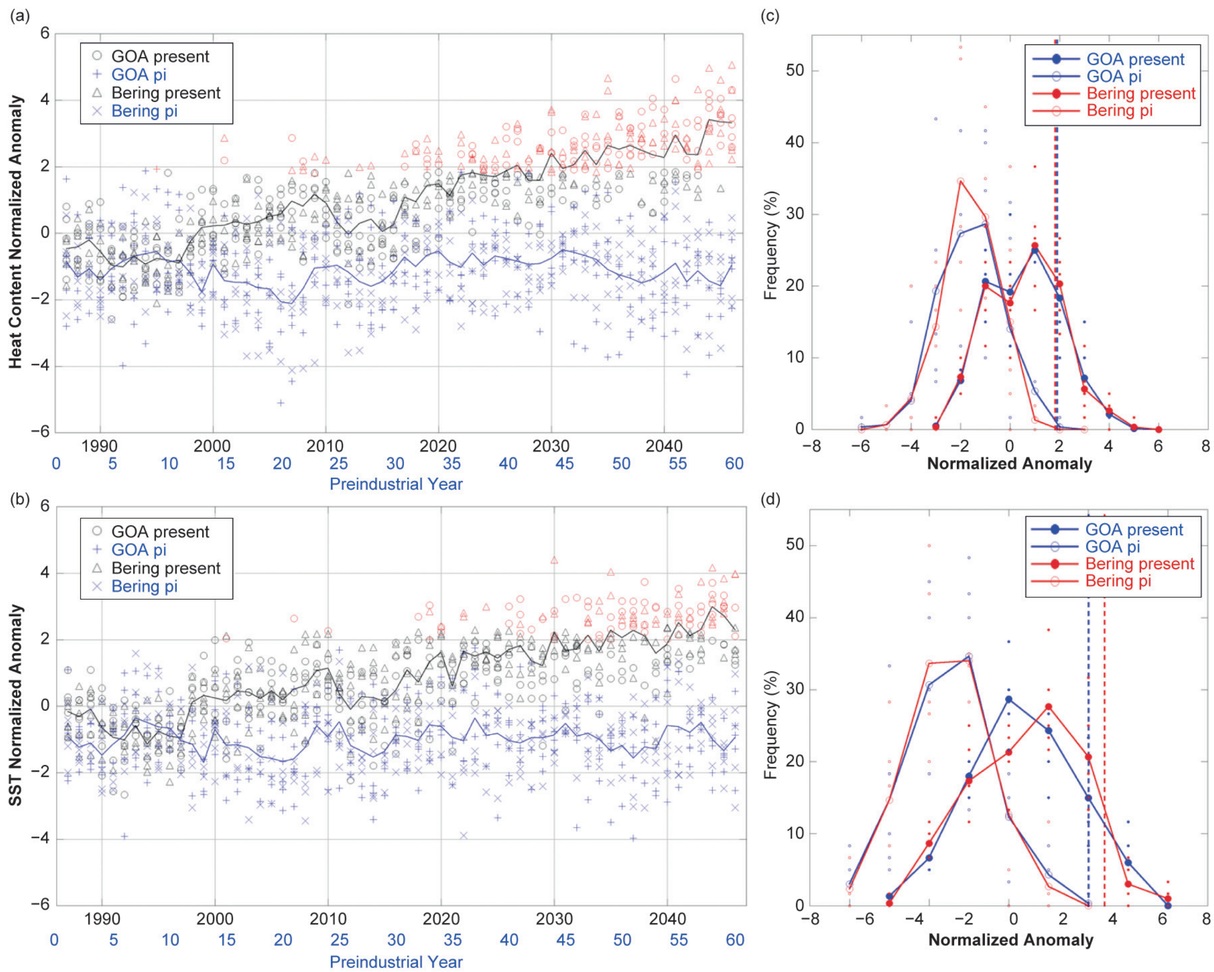

Fig. 8.2. Normalized anomalies of (a) heat content and (b) SSTs for the present (black) and preindustrial (blue) climate of the GOA (circle and plus) and Bering Sea (triangle and x) regions from the five model ensembles. Anomalies exceeding 2016 value are in red (shapes as indicated), and the ensemble/region means are shown by the solid lines. Mean probability distributions (%) of (c) heat content and (d) SSTs from the model ensembles; solid (open) circles indicate present (preindustrial) climate for the GOA (blue) and Bering Sea (red). Spread of individual models is shown by the smaller, corresponding open/closed circles. Dashed vertical lines show the 2016 anomalies: GOA (blue), Bering Sea (red).

generally cooler with no extreme positive anomalies comparable to the present climate (Figs. 8.2c,d).

Each model/variable/region was compared with its corresponding 2016 observed normalized anomaly value (see red coloring in Figs. 8.2a,b and vertical dashed lines in Figs. 8.2c,d). The preindustrial period had few cases meeting or exceeding the 2016 anomaly for any region or variable, while the present climate had many more, especially later in the period. For HC the number of years each model exceeded the 2016 anomaly ranged from 11 to 20 (0–2) cases in the present (preindustrial) climate for GOA and 16–24 (0) for Bering Sea. Fewer cases reached 2016 values in SSTs, with 5–18 (0–1) for GOA and 4–11 (0) for Bering Sea. For both variables the Bering Sea region's preindustrial climate never reached the 2016 observed magnitude.

In this analysis the fraction of attributable risk (FAR; Stott et al. 2004; NASEM 2016) was computed as FAR = 1 – $Prob_{preindustrial}/Prob_{present}$ with the probability being the exceedance of the observed 2016 normalized anomaly. Bering Sea SSTs had FAR = 1 for all cases, while the GOA's FARs were 0.88–1 for SST and 0.82–1 for HC (but most models had FAR = 1, i.e., no instances of 2016-like anomalies in the preindustrial climate).

Conclusion. The warmth of the Bering Sea in 2016 was unprecedented in the historical record, and the warmth of the GOA nearly so. The FAR values based on an ensemble of five global climate models indicate that the 2016 warm ocean anomalies cannot be explained without anthropogenic climate warming, although the region's large internal variability was also a contributing factor (Fig. 8.1 and online supplement material). A strong El Niño with a positive PDO (warm) phase, together with preconditioning of the waters during 2014/15 and the anomalous atmospheric circulation of early 2016, made for a "perfect storm" of marine heating around Alaska. Both anthropogenic forcing and internal variability were necessary for the extreme warmth of the subarctic seas. Our conclusions are consistent with and extend previous findings concerning the 2014 warm SST anomalies in the northeast Pacific (Weller et al. 2015). Additionally, the trajectory of the present climate with RCP8.5 indicates that SST and HC extreme anomalies like 2016 will become common in the coming decades. Given the many impacts of the 2016 anomaly, the future climate projected here will result in a profound shift for people, systems, and species when such warm ocean temperatures become common and not extreme in the GOA and Bering regions.

ACKNOWLEDGMENTS. This work was supported by the Alaska Climate Science Center through Cooperative Agreement G10AC00588 from the USGS and by the NOAA Climate Program Office through Grant NA16OAR4310162 to the Alaska Center for Climate Assessment and Policy. The papers contents are solely the responsibility of the authors and do not necessarily represent the official views of the USGS.

REFERENCES

Bond, N. A., M. F. Cronin, H. Freeland, and N. Mantua 2015: Causes and impacts of the 2014 warm anomaly in the NE Pacific. *Geophys. Res. Lett.,* **42**, 3414–3420, doi:10.1002/2015GL063306.

Di Lorenzo, E., and N. Mantua, 2016: Multi-year persistence of the 2014/15 North Pacific marine heatwave. *Nat. Climate Change*, **6**, 1042–1047, doi:10.1038/nclimate3082.

Freeland, H., 2014: Something odd in the Gulf of Alaska, February 2014. *CMOS Bulletin SCMO*, **42**, 57–59. [Available online at http://cmos.ca/uploaded/web/members/Bulletin/Vol_42/b4202.pdf.]

Huang, B., and Coauthors, 2014: Extended reconstructed sea surface temperature version 4 (ERSST.v4): Part I. Upgrades and intercomparisons. *J. Climate*, **28**, 911–930, doi:10.1175/JCLI-D-14-00006.1

Lee, M.-Y., C.-C. Hong and H.-H. Hsu, 2015: Compounding effects of warm sea surface temperature and reduced sea ice extent on the extreme circulation over the extratropical North Pacific and North America during the 2013-2014 boreal winter. *Geophys. Res. Lett.*, **42**, 1612–1618, doi:10.1002/2014GL062956.

Kintisch, E., 2015: 'The Blob' invades Pacific, flummoxing climate experts. *Science*, **348**, 17–18.

NASEM, 2016*: Attribution of extreme weather events in the context of climate change*. National Academies Press, 186 pp., doi:10.17226/21852.

Peterson, W., N. Bond, and M. Robert, 2016a: The blob (part three): Going, going, gone? *PICES Press*, **24** (1), 46–48. [Available online at https://pices.int/publications/pices_press/volume24/PPJan2016.pdf.]

——, ——, and ——, 2016b: The blob is gone but has morphed into a strongly positive PDO/SST pattern. *PICES Press*, **24** (2), 46–47, 50. [Available online at http://meetings.pices.int/publications/pices-press/volume24/issue2/PPJuly2016.pdf.]

Roemmich, D., and J. Gilson, 2009: The 2004–2008 mean and annual cycle of temperature, salinity, and steric height in the global ocean from the Argo Program. *Progr. Oceanogr.,* **82**, 81–100, doi:10.1016/j.pocean.2009.03.004.

Saha, S., and Coauthors, 2006: The NCEP climate forecast system. *J. Climate,* **19**, 3483–3517, doi:10.1175/JCLI3812.1.

Seager, R., M. Hoerling, S. Schubert, H. Wang, B. Lyon, A. Kumar, J. Nakamura, and N. Henderson, 2015: Causes of the 2011–14 California drought. *J. Climate*, **28**, 6997–7024, doi:10.1175/JCLI-D-14-00860.1.

Stott, P., D. Stone, and M. Allen, 2004: Human contribution to the European heatwave of 2003. *Nature*, **432**, 610–614, doi:10.1038/nature03089.

Walsh, J. E., P. A. Bieniek, B. Brettschneider, E. S. Euskirchen, R. Lader, and R. L. Thoman, 2017: The exceptionally warm winter of 2015-16 in Alaska: Attribution and anticipation. *J. Climate*, **30**, 2069–2088, doi:10.1175/JCLI-D-16-0473.1.

Weller, E., S.-K. Min, D. Lee, W. Cai, S.-W. Yeh, and J.-S. Kug, 2015: Human contribution to the 2014 record high sea surface temperatures over the western tropical and northeast Pacific Ocean [in "Explaining Extreme Events of 2014 from a Climate Perspective"]. *Bull. Amer. Meteor. Soc.,* **96** (12), S100–S104, doi:10.1175/BAMS-D-15-00055.1.

Table 1.1. SUMMARY of RESULTS

	ANTHROPOGENIC INFLUENCE ON EVENT		
	INCREASE	**DECREASE**	**NOT FOUND OR UNCERTAIN**
Heat	Ch. 3: Global Ch. 7: Arctic Ch. 15: France Ch. 19: Asia		
Cold		Ch. 23: China Ch. 24: China	
Heat & Dryness	Ch. 25: Thailand		
Marine Heat	Ch. 4: Central Equatorial Pacific Ch. 5: Central Equatorial Pacific Ch. 6: Pacific Northwest Ch. 8: North Pacific Ocean/Alaska Ch. 9: North Pacific Ocean/Alaska Ch. 9: Australia		Ch. 4: Eastern Equatorial Pacific
Heavy Precipitation	Ch. 20: South China Ch. 21: China (Wuhan) Ch. 22: China (Yangtze River)		Ch. 10: California (failed rains) Ch. 26: Australia Ch. 27: Australia
Frost	Ch. 29: Australia		
Winter Storm			Ch. 11: Mid-Atlantic U.S. Storm "Jonas"
Drought	Ch. 17: Southern Africa Ch. 18: Southern Africa		Ch. 13: Brazil
Atmospheric Circulation			Ch. 15: Europe
Stagnant Air			Ch. 14: Western Europe
Wildfires	Ch. 12: Canada & Australia (Vapor Pressure Deficits)		
Coral Bleaching	Ch. 5: Central Equatorial Pacific Ch. 28: Great Barrier Reef		
Ecosystem Function		Ch. 5: Central Equatorial Pacific (Chl-***a*** and primary production, sea bird abundance, reef fish abundance) Ch. 18: Southern Africa (Crop Yields)	
El Niño	Ch. 18: Southern Africa		Ch. 4: Equatorial Pacific (Amplitude)
TOTAL	18	3	9

	METHOD USED	Total Events
Heat	Ch. 3: CMIP5 multimodel coupled model assessment with piCont, historicalNat, and historical forcings Ch. 7: CMIP5 multimodel coupled model assessment with piCont, historicalNat, and historical forcings Ch. 15: Flow analogues conditional on circulation types Ch. 19: MIROC-AGCM atmosphere only model conditioned on SST patterns	
Cold	Ch. 23: HadGEM3-A (GA6) atmosphere only model conditioned on SST and SIC for 2016 and data fitted to GEV distribution Ch. 24: CMIP5 multimodel coupled model assessment	
Heat & Dryness	Ch. 25: HadGEM3-A N216 Atmosphere only model conditioned on SST patterns	
Marine Heat	Ch. 4: SST observations; SGS and GEV distributions; modeling with LIM and CGCMs (NCAR CESM-LE and GFDL FLOR-FA) Ch. 5: Observational extrapolation (OISST, HadISST, ERSST v4) Ch. 6: Observational extrapolation; CMIP5 multimodel coupled model assessment Ch. 8: Observational extrapolation; CMIP5 multimodel coupled model assessment Ch. 9: Observational extrapolation; CMIP5 multimodel coupled model assessment	
Heavy Precipitation	Ch. 10: CAM5 AMIP atmosphere only model conditioned on SST patterns and CESM1 CMIP single coupled model assessment Ch. 20: Observational extrapolation; CMIP5 and CESM multimodel coupled model assessment; auto-regressive models Ch. 21: Observational extrapolation; HadGEM3-A atmosphere only model conditioned on SST patterns; CMIP5 multimodel coupled model assessment with ROF Ch. 22: Observational extrapolation, CMIP5 multimodel coupled model assessment Ch. 26: BoM seasonal forecast attribution system and seasonal forecasts Ch. 27: CMIP5 multimodel coupled model assessment	
Frost	Ch. 29: *weather@home* multimodel atmosphere only models conditioned on SST patterns; BoM seasonal forecast attribution system	
Winter Storm	Ch. 11: ECHAM5 atmosphere only model conditioned on SST patterns	
Drought	Ch. 13: Observational extrapolation; weather@home multimodel atmosphere only models conditioned on SST patterns; HadGEM3-A and CMIP5 multimodel coupled model assessent; hydrological modeling Ch. 17: Observational extrapolation; CMIP5 multimodel coupled model assessment; VIC land surface hdyrological model, optimal fingerprint method Ch. 18: Observational extrapolation; *weather@home* multimodel atmosphere only models conditioned on SSTs, CMIP5 multimodel coupled model assessment	
Atmospheric Circulation	Ch. 15: Flow analogues distances analysis conditioned on circulation types	
Stagnant Air	Ch. 14: Observational extrapolation; Multimodel atmosphere only models conditioned on SST patterns including: HadGEM3-A model; EURO-CORDEX ensemble; EC-EARTH+RACMO ensemble	
Wildfires	Ch. 12: HadAM3 atmospere only model conditioned on SSTs and SIC for 2015/16	
Coral Bleaching	Ch. 5: Observations from NOAA Pacific Reef Assessment and Monitoring Program surveys Ch. 28: CMIP5 multimodel coupled model assessment; Observations of climatic and environmental conditions (NASA GES DISC, HadCRUT4, NOAA OISSTV2)	
Ecosystem Function	Ch. 5: Observations of reef fish from NOAA Pacific Reef Assessment and Monitoring Program surveys; visual observations of seabirds from USFWS surveys. Ch. 18: Empirical yield/rainfall model	
El Niño	Ch. 4: SST observations; SGS and GEV distributions; modeling with LIM and CGCMs (NCAR CESM-LE and GFDL FLOR-FA) Ch. 18: Observational extrapolation; *weather@home* multimodel atmosphere only models conditioned on SSTs, CMIP5 multimodel coupled model assessment	
		30